

# Non-Fickian diffusion and tau approximation from numerical turbulence

Axel Brandenburg\*

*NORDITA, Blegdamsvej 17, DK-2100 Copenhagen Ø, Denmark*

Petri J. Käpylä†

*Kiepenheuer-Institut für Sonnenphysik, Schöneckstraße 6, D-79104 Freiburg, Germany and  
Department of Physical Sciences, Astronomy Division,  
P.O. Box 3000, FIN-90014 University of Oulu, Finland*

Amjed Mohammed‡

*Physics Department, Oldenburg University, 26111 Oldenburg, Germany*

(Dated: October 30, 2018, Revision: 1.57 )

Evidence for non-Fickian diffusion of a passive scalar is presented using direct simulations of homogeneous isotropic turbulence. The results compare favorably with an explicitly time-dependent closure model based on the tau approximation. In the numerical experiments three different cases are considered: (i) zero mean concentration with finite initial concentration flux, (ii) an initial top hat profile for the concentration, and (iii) an imposed background concentration gradient. All cases agree in the resulting relaxation time in the tau approximation relating the triple correlation to the concentration flux. The first order smoothing approximation is shown to be inapplicable.

PACS numbers: 44.25.+f, 47.27.Eq, 47.27.Gs, 47.27.Qb

## I. INTRODUCTION

In a turbulent flow the transport of a passive scalar is an important problem in atmospheric research, astrophysics, and combustion [1, 2]. Passive scalar transport is also an important benchmark for more complicated turbulent transport processes such as turbulent magnetic diffusion and the alpha-effect in dynamo theory [3, 4], or turbulent viscosity and its nondiffusive counterparts such as the AKA-effect [5, 6] and the Lambda effect [7, 8].

Modeling turbulent transport in terms of turbulent diffusion is known to have major deficiencies. For example turbulent transport is known to be anomalous, i.e. the width  $\sigma$  of a localized patch of passive scalar concentration may expand in time like  $\sigma^2 \sim t^\beta$ , where  $\beta = 1$  corresponds to ordinary (Brownian) diffusion,  $\beta > 1$  is superdiffusion, and  $\beta < 1$  is subdiffusion [9]. Thermal convection, for example, has superdiffusive properties [10]. Turbulent transport is also known to have nonlocal and nondiffusive properties. One of the outcomes of this realization was the development of the transient matrix approach [11, 12] which captures nonlocal transport properties, although only in a diagnostic fashion [10]. In order to describe nonlocal aspects in a prognostic fashion, higher order spatial derivatives of the turbulent fluxes need to be included. These are best incorporated in terms of an integral kernel [13].

In the present work, however, instead of invoking higher order spatial derivatives, we follow the recent

proposal of Blackman and Field [14, 15] to include an additional second order *time derivative* instead. This turns the diffusion equation into a damped wave equation. Blackman and Field derived this equation from turbulent mean field theory by retaining triple correlations in the transport equation for the mean flux of a passive scalar. They assumed an isotropic turbulent flow and use a closure which relates triple correlations to double correlations [16, 17, 18, 19]. This approach is in some ways more elegant than the classical first order smoothing approximation [3, 4, 20], which breaks down because it assumes that the triple correlations are simply negligible. This approach also incorporates the momentum equation and, in magnetohydrodynamics, it therefore allows a natural derivation of the feedback term of the alpha effect in magnetohydrodynamics [14, 19].

Adding an extra time derivative in the equation for the turbulent transport of a passive scalar does certainly solve another long standing problem. Solutions to the diffusion equation are known to violate causality, because the diffusion equation is elliptic and the propagation speed of a signal is infinite [21]. This problem was originally discussed in the context of general relativity [22], and more recently in the context of black hole accretion [23, 24]. The extra time derivative affects the modeling of turbulent transport most strongly at early times, just after having injected the passive scalar. This additional time derivative term tends to make the turbulent transport more ballistic at early times (corresponding to  $\beta \approx 2$ ). This property is well known in the context of standard Brownian motion.

Non-Fickian diffusion has previously also been discussed in various engineering applications, for example in diffusion problems in composite media [25, 26] and in neutron transport problems in reactors [27], which

\*Electronic address: brandenb@nordita.dk

†Electronic address: petri.kapyla@oulu.fi

‡Electronic address: amjed@mail.uni-oldenburg.de

are best modeled using non-Fickian diffusion. Here, a non-Fickian diffusion equation for particle transport arises by taking moments of the one dimensional Kramers equation, and approximating the second moment by the Maxwellian value [26, 28]. In these applications, however, turbulence is not considered. One exception is the recent work of Ghosal and Keller [29] who derived a non-Fickian diffusion equation with the extra time derivative by going to the next higher order in an expansion of the underlying integral equation. Comparing with data on smoke plumes in the atmosphere and on heat flow in a wind tunnel they find improved agreement with non-Fickian diffusion at small distances from the source.

Given that the diffusion equation is now turned into a damped wave equation, one wonders whether oscillatory behavior is possible. Blackman and Field [15] find that oscillatory behavior is indeed present for long enough damping times but disappears for short damping times. For diffusion of a mean passive scalar, they argue that the oscillatory behavior is likely unphysical, and they use this to constrain their damping time to be of order of the eddy turnover time. However, the different numerical experiments presented below suggest that the damping time is about three times longer than the eddy turnover time. Furthermore, the simulations give direct evidence for mildly oscillatory behavior in a certain parameter regime.

The objective of the present paper is twofold. First we need to find out whether the existence of the proposed additional time derivative can actually be confirmed using turbulence simulations. If so, we need to find out the magnitude of this extra term. Second, we need to study the range of modifications expected from this new term. In order to do this we consider numerical simulations of weakly compressible turbulence including the transport of a passive scalar.

We begin by discussing the formalism that leads to the emergence of the additional time derivative in mean field theory. We then discuss the type of simulations carried out and present three numerical experiments that quantify the relative importance of the additional time derivative and that support the tau approximation formalism.

## II. FIRST ORDER SMOOTHING VERSUS TAU APPROXIMATION

A classic application of passive scalar transport is the diffusion of smoke in a turbulent atmosphere. If the smoke is injected in one point it will diffuse radially outward, so the mean concentration is expected to be a function of radius  $r$  and time  $t$ . In that case it makes sense to consider averages over spherical shells, i.e.

$$\overline{C}(r, t) \equiv \frac{1}{4\pi} \int_0^{2\pi} \int_0^\pi C(r, \theta, \phi, t) \sin \theta \, d\theta \, d\phi, \quad (1)$$

where  $C$  is the concentration per unit volume. Another application is the passive scalar diffusion between two parts of a slab that are initially separated by a membrane. In that case the mean concentration varies along the direction of the slab, say  $z$ , and then it makes sense to define horizontal averages, i.e.

$$\overline{C}(z, t) \equiv \frac{1}{L_x L_y} \int_0^{L_x} \int_0^{L_y} C(x, y, z, t) \, dx \, dy. \quad (2)$$

This is also the type of average that is best suited for studies in cartesian geometry considered here.

For clarity of the presentation here we ignore microscopic diffusion, in which case  $C$  satisfies the simple conservation equation,

$$\frac{\partial C}{\partial t} = -\nabla \cdot (\mathbf{U}C), \quad (3)$$

where  $\mathbf{U}$  is the fluid velocity. The effects of finite microscopic diffusion will be discussed in the appendix. We now split  $\mathbf{U}$  and  $C$  into mean and fluctuating parts, i.e.

$$\mathbf{U} = \overline{\mathbf{U}} + \mathbf{u}, \quad C = \overline{C} + c, \quad (4)$$

and average Eq. (3), so we have

$$\frac{\partial \overline{C}}{\partial t} = -\nabla \cdot (\overline{\mathbf{U}}\overline{C} + \overline{\mathbf{u}c}). \quad (5)$$

The challenge is now to find an expression for the concentration flux,  $\overline{\mathbf{u}c} \equiv \overline{\mathcal{F}}$  in terms of the mean concentration,  $\overline{C}$ . The standard approach is to express the departure of the concentration from its average,  $c \equiv C - \overline{C}$ , in terms of its past evolution, i.e.

$$c(\mathbf{x}, t) = \int_0^t \dot{c}(\mathbf{x}, t') \, dt', \quad (6)$$

where the dot denotes time differentiation and

$$\dot{c} \equiv \dot{C} - \dot{\overline{C}} = -\nabla \cdot (\overline{\mathbf{U}}c + \mathbf{u}\overline{C} + \mathbf{u}c - \overline{\mathbf{u}c}) \quad (7)$$

is the evolution equation for the passive scalar fluctuation obtained by subtracting Eq. (5) from (3). In the first order smoothing approximation or, which is the same, the quasilinear or second order correlation approximation [7], one *ignores* the terms that are nonlinear in the fluctuations, i.e. the terms  $\mathbf{u}c - \overline{\mathbf{u}c}$  in Eq. (7) are simply omitted [3, 4]. This is only justified if microscopic diffusion is large (but we have already assumed it to be negligible) or if the velocity is delta-correlated in time (which is also unrealistic).

The terms that are nonlinear in the fluctuations would lead to triple correlations of the form  $\overline{u_i u_j \partial_j c}$ . Various authors have proposed to approximate triple correlations by quadratic correlations [14, 16, 17, 18, 19] which, in the present case, would be  $\overline{u_i c} / \tau$ ; see Ref. [15]. This is reminiscent of the Eddy-Damped Quasi-Normal Markovian approximation [30, 31], where fourth order correlations are approximated by third order correlations. This is

normally referred to as the tau approximation. In order to distinguish the two approaches, Blackman and Field [15] call the approach used in Refs [14, 16, 17, 18, 19] the “minimal tau approximation”. In these approaches one calculates not  $\overline{\mathcal{F}}$ , but instead its time derivative. In that case the time integration in Eq. (7) disappears and one has

$$\frac{\partial \overline{\mathcal{F}}}{\partial t} = \overline{\mathbf{u}(\mathbf{x}, t) \dot{c}(\mathbf{x}, t)} + \overline{\dot{\mathbf{u}}(\mathbf{x}, t) c(\mathbf{x}, t)}. \quad (8)$$

This leads to the final equation

$$\frac{\partial \overline{\mathcal{F}}_i}{\partial t} = -\overline{u_i u_j} \partial_j \overline{C} - \frac{\overline{\mathcal{F}}_i}{\tau}, \quad (9)$$

where  $\tau$  is some relaxation time and incompressibility has been assumed, i.e.  $\partial_j u_j = 0$ . We shall now also assume isotropy,  $\overline{u_i u_j} = \frac{1}{3} \delta_{ij} u_{\text{rms}}^2$ , where  $u_{\text{rms}}$  is the rms velocity with  $u_{\text{rms}}^2 = \overline{\mathbf{u}^2}$ . The validity of Eq. (9) is clearly something that ought to be checked numerically using turbulence simulations. This is the main objective of the present paper.

The other aspect is that the time derivative may not be ignorable in the final set of evolution equations. Thus, in contrast to ordinary Fickian diffusion, where the passive scalar flux  $\overline{\mathcal{F}}$  is assumed to be proportional to the mean negative concentration gradient (Fick’s law), i.e.

$$\overline{\mathcal{F}} = -\kappa_t \nabla \overline{C} \quad (\text{Fickian diffusion}), \quad (10)$$

where  $\kappa_t = \frac{1}{3} \tau_{\text{cor}} u_{\text{rms}}^2$  is the turbulent passive scalar diffusivity and  $\tau_{\text{cor}}$  is some correlation time, one now has [15]

$$\overline{\mathcal{F}} = -\kappa_t \nabla \overline{C} - \tau \frac{\partial \overline{\mathcal{F}}}{\partial t} \quad (\text{non-Fickian}), \quad (11)$$

where  $\kappa_t = \frac{1}{3} \tau u_{\text{rms}}^2$ . Equation (10) can be reconciled only when time variations of the concentration flux have become small and if the correlation time  $\tau_{\text{cor}}$  is identified with the damping time  $\tau$ .

Applying  $\partial_t + \tau^{-1}$  on both sides of (5), ignoring for simplicity a mean flow ( $\overline{\mathbf{U}} = 0$ ), and inserting (11) yields a damped wave equation,

$$\frac{\partial^2 \overline{C}}{\partial t^2} + \frac{1}{\tau} \frac{\partial \overline{C}}{\partial t} = \frac{1}{3} u_{\text{rms}}^2 \nabla^2 \overline{C}. \quad (12)$$

We note in passing that the extra term is in some ways analogous to the displacement current in the Maxwell equations. This is why this equation is also known in the literature as the Cattaneo–Maxwell equation [32]. The maximum signal speed is limited by  $u_{\text{rms}}/\sqrt{3}$ . Assessing the importance of the extra time derivative is another objective of the present paper.

The only ill-known free parameter in this theory is  $\tau$ , whose value is conveniently expressed in terms of the Strouhal number [4],

$$\text{St} = \tau u_{\text{rms}} k_f, \quad (13)$$

where  $k_f$  is the forcing wavenumber or, more generally, the wavenumber of the scale of the energy carrying eddies. Here and elsewhere we consider  $u_{\text{rms}}$  as a constant (independent of  $z$  and  $t$ ).

Some preliminary estimate of St can be made by considering the late time behavior where Fickian diffusion holds. From Eq. (10) we expect that the decay rate of a large scale pattern with wavenumber  $k_1$  is

$$\lambda_c = \kappa_t k_1^2, \quad (14)$$

where  $\kappa_t = \frac{1}{3} \tau u_{\text{rms}}^2$  is the turbulent diffusion coefficient. From forced turbulence simulations with initial mean flow or mean magnetic field patterns [33], the decay rates of these patterns are well described by a turbulent kinematic viscosity,  $\nu_t$ , and a turbulent magnetic diffusion coefficient,  $\eta_t$ , where both coefficients are about equally large with

$$\nu_t \approx \eta_t \approx (0.8 \dots 0.9) \times u_{\text{rms}}/k_f. \quad (15)$$

Applying the same value also to  $\kappa_t$  we obtain

$$\text{St} \approx (0.8 \dots 0.9) \times 3 = 2.4 \dots 2.7. \quad (16)$$

This result is remarkable in view of the fact that in the classic first order smoothing approach to turbulent transport coefficients one has to assume  $\text{St} \ll 1$ ; see Refs [4, 20].

### III. COMPARISON WITH SIMULATIONS

In order to test the viability of the non-Fickian diffusion approach and to determine the value of St we have designed three different types of turbulence simulations. We first consider the problem of a finite initial flux,  $\overline{\mathcal{F}}$ , but with zero mean concentration,  $\overline{C} = 0$  [15]. Next we consider the evolution of an initial top hat profile for  $C$  and finally we investigate the case of an imposed uniform gradient of  $C$  which leads to the most direct determination of  $\tau$  as a function of Reynolds number and forcing wavenumber. We begin with a brief description of the simulations carried out.

#### A. Summary of the type of simulations

We consider subsonic turbulence in an isothermal gas with constant sound speed  $c_s$  in a periodic box of size  $2\pi \times 2\pi \times 2\pi$ . The Navier–Stokes equation for the velocity  $\mathbf{U}$  is written in the form

$$\frac{D\mathbf{U}}{Dt} = -c_s^2 \nabla \ln \rho + \mathbf{F}_{\text{visc}} + \mathbf{f}, \quad (17)$$

where  $\rho$  is the density,  $D/Dt = \partial/\partial t + \mathbf{U} \cdot \nabla$  is the advective derivative,

$$\mathbf{F}_{\text{visc}} = \nu (\nabla^2 \mathbf{U} + \frac{1}{3} \nabla \nabla \cdot \mathbf{U} + 2\mathbf{S} \cdot \nabla \ln \rho) \quad (18)$$

is the viscous force where  $\nu = \text{const}$  is the kinematic viscosity,  $S_{ij} = \frac{1}{2}(U_{i,j} + U_{j,i}) - \frac{1}{3}\delta_{ij}U_{k,k}$  is the traceless rate of strain tensor, and  $\mathbf{f}$  is a random forcing function (see below). The continuity equation is

$$\frac{\partial \rho}{\partial t} = -\nabla \cdot (\mathbf{U}\rho), \quad (19)$$

and the equation for the passive scalar concentration per unit volume,  $C$ , is

$$\frac{\partial C}{\partial t} = -\nabla \cdot \left[ \mathbf{U}C - \rho\kappa_C \nabla \left( \frac{C}{\rho} \right) \right], \quad (20)$$

where  $\kappa_C = \text{const}$  is the diffusion coefficient for the passive scalar concentration, which is related to  $\nu$  by the Schmidt number,

$$\text{Sc} = \nu/\kappa_C. \quad (21)$$

Throughout this work we take  $\text{Sc} = 1$ . A nondimensional measure of  $\nu$  and hence  $\kappa_C$  is the Reynolds number, which is here defined with respect to the inverse forcing wavenumber,

$$\text{Re} = u_{\text{rms}}/(\nu k_f). \quad (22)$$

The maximum possible value of  $\text{Re}$  depends on the resolution and the value of  $k_f$ . For  $k_f = 1.5$  the typical value is approximately equal to the number of meshpoints in one direction.

We adopt a forcing function  $\mathbf{f}$  of the form

$$\mathbf{f}(\mathbf{x}, t) = \text{Re}\{N\mathbf{f}_{\mathbf{k}(t)} \exp[i\mathbf{k}(t) \cdot \mathbf{x} + i\phi(t)]\}, \quad (23)$$

where  $\mathbf{x} = (x, y, z)$  is the position vector, and  $-\pi < \phi(t) < \pi$  is a ( $\delta$ -correlated) random phase. The normalization factor is  $N = f_0 c_s (kc_s/\delta t)^{1/2}$ , with  $f_0$  a nondimensional forcing amplitude,  $k = |\mathbf{k}|$ , and  $\delta t$  the length of the time step; we chose  $f_0 = 0.05$  so that the maximum Mach number stays below about 0.5 (the rms Mach number is close to 0.2 in all runs [36]). The vector amplitude  $\mathbf{f}_{\mathbf{k}}$  describes nonhelical transversal waves with  $|\mathbf{f}_{\mathbf{k}}|^2 = 1$  and

$$\mathbf{f}_{\mathbf{k}} = (\mathbf{k} \times \mathbf{e}) / \sqrt{k^2 - (\mathbf{k} \cdot \mathbf{e})^2}, \quad (24)$$

where  $\mathbf{e}$  is an arbitrary unit vector. At each time step we select randomly one of many possible wave vectors in a finite range around the forcing wavenumber  $k_f$  (see below).

The equations are solved using the same method as in Ref. [37], but here we employ a new cache and memory efficient code [38] using MPI (Message Passing Interface) library calls for communication between processors. This allows us to run at a resolutions up to  $1024^3$  meshpoints [39, 40].

## B. Finite initial flux experiment

We consider first the example discussed by Blackman and Field [15]. In Fickian diffusion, if  $\overline{C} = 0$ , there should be no flux, i.e.  $\overline{\mathcal{F}} = 0$ . Although this should in general be correct, one can imagine contrived situations where this is not the case, so it is an ideal problem to test whether the inclusion of the extra time derivative of the flux is at all correct and meaningful. Without this extra time derivative  $\overline{C}$  would always stay zero.

To explain in simple terms what happens, consider a situation where we have initially uniformly mixed white and black balls (so  $\overline{C} = 0$ ), but for some reason the balls are given an initial push such that the white balls move to the right part of the domain and all the black balls move to the left part of the domain. Then, after a short time, there should be a systematic segregation of white and black balls, in spite of continuous random forcing. Of course, this segregation survives only for a dynamical time, after which ordinary diffusion will begin to mix white and black balls.

In order to set up such a situation in a turbulence simulation we assume that at  $t = 0$  the turbulence has already fully developed and then we initialize the passive scalar distribution according to

$$C(x, y, z, 0) = C_0 \frac{u_z(x, y, z, 0)}{u_{\text{rms}}} \sin k_1 z. \quad (25)$$

Since  $\overline{u_z} = 0$ , and since the Reynolds rules [4] are obeyed by our horizontal averages, we have  $\overline{C}(z, 0) = 0$ , but because  $\overline{u_z^2} \neq 0$ , we have  $\overline{\mathcal{F}_z} = \overline{u_z c} \neq 0$ .

Numerically, we monitor the evolution of  $\langle \overline{C^2} \rangle^{1/2}$ , where angular brackets denote an average over  $z$ . This is to be compared with the analytic solution of the model equation (12). Assuming that  $\overline{C}(z, t)$  is proportional to  $\exp(ik_1 z + \lambda t)$ , the two eigenvalues are

$$\lambda_{\pm}(k_1) = -\lambda_0 \pm \Delta\lambda(k_1), \quad (26)$$

where

$$\lambda_0 = \frac{u_{\text{rms}} k_f}{2 \text{St}}, \quad \Delta\lambda(k_1) = \sqrt{\lambda_0^2 - \frac{1}{3} u_{\text{rms}}^2 k_1^2}. \quad (27)$$

The solution that satisfies  $\overline{C}(z, 0) = 0$  is

$$\langle \overline{C^2} \rangle^{1/2} = A \exp(-\lambda_0 t) \sinh(\Delta\lambda t), \quad (28)$$

where  $A$  is an amplitude factor. Oscillatory solutions are possible ( $\Delta\lambda$  imaginary) either when  $\text{St}$  is large enough or, since  $\text{St}$  cannot be manipulated in a simulation, when  $k_f$  is small enough. According to Eq. (16) we can estimate

$$k_f/k_1 < 2 \text{St}/\sqrt{3} \approx 3 \quad (\text{oscillatory behavior}). \quad (29)$$

In the oscillatory case,  $\Delta\lambda$  is imaginary and so  $\langle \overline{C^2} \rangle^{1/2}$  is proportional to  $e^{-\lambda_0 t} |\sin \omega t|$ , where  $\omega = \text{Im} \Delta\lambda$ .

Note that the solution depends only on the combination  $\text{St}/k_f$ , where  $k_f$  should be a known input parameter

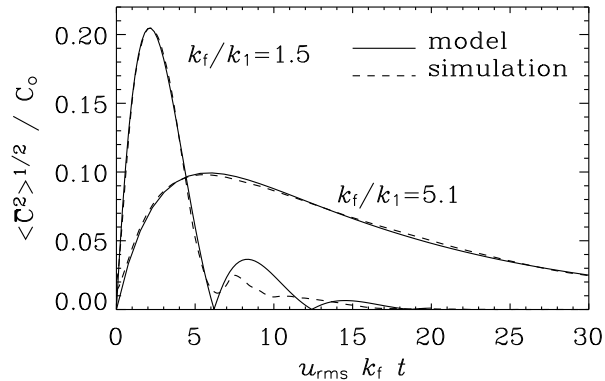


FIG. 1: Passive scalar amplitude,  $\langle C^2 \rangle^{1/2}/C_0$ , versus time (normalized by  $u_{\text{rms}} k_f$ ) for two different values of  $k_f/k_1$ . The simulations have  $256^3$  meshpoints. The results are compared with solutions to the non-Fickian diffusion model.

TABLE I: Summary of fit parameters for the finite initial flux experiment. In all cases, the measured value of  $u_{\text{rms}} = 0.23$  is used. Note that  $k_f^{(\text{fit})}$  is an independent fit parameter used instead of  $k_f$  to model the solution for a given value of  $k_f$ . The range of wavenumbers used in the forcing function is also given.

$k_f/k_1$	(range)	$k_f^{(\text{fit})}/k_1$	$\text{St}^{(\text{fit})}$	$A^{(\text{fit})}$
1.5	(1...2)	1.0	1.8	0.21
2.2	(2...3)	1.6	1.8	0.38
5.1	(4.5...5.5)	3.8	2.4	0.18

for a given simulation. However, in order to be able to fit the model to the simulation we have considered  $\text{St}$  and  $k_f$  as independent fit parameters and refer then to the quantity  $k_f^{(\text{fit})}$ . The results of our fits of the simulations to the models are shown in Fig. 1. The corresponding fit parameters are listed in Table I.

We see that in all cases the Strouhal number does indeed exceed unity. The resulting value is close to the value based on our simple estimate in Eq. (16). Second, oscillatory behavior of the solution is not only mathematically possible for small values of  $k_f$ , see Eq. (26), but it is even physically realized in the solution for  $k_f/k_1 = 1.5$ .

### C. Initial top hat function

Next we consider the problem of an initial step function. The advantage of such a profile as initial condition is that a broad spectrum of wavenumbers is excited. In order to avoid sharp jumps in the initial condition we choose a smoothed top hat function using the initial pro-

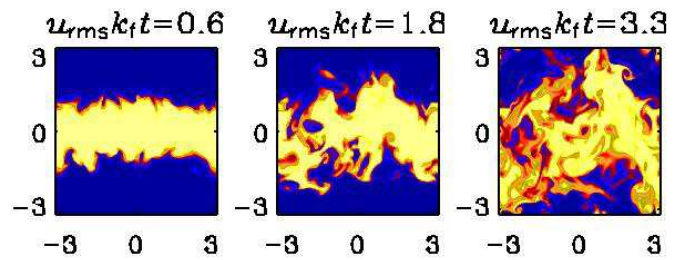


FIG. 2:  $C(x, 0, z)$  at three different times after reinitializing  $C$  according to Eq. (30).  $k_f/k_1 = 1.5$ ,  $\text{Re}_{\text{LS}} = 400$ .

file

$$C(x, y, z, 0) = \frac{1}{2} + \frac{1}{2} \tanh[k_z^2(d^2 - z^2)], \quad (30)$$

where  $k_z = 2$  and  $d = 1$  throughout this work.

It is important to start the experiment at a time when the turbulence is fully developed. A visualization of  $C$  at three different times after reinitializing  $C$  is shown in Fig. 2.

For Fickian diffusion the initial top hat function will broaden and develop eventually into a gaussian. As usual, for large enough values of the Strouhal number, wave-like behavior is possible and this would correspond to the initial bump splitting up into two bumps traveling in opposite directions. We have not been able to see this in our simulations so far. We have therefore decided to introduce as a quantitative measure of the departure from a gaussian profile the kurtosis,

$$\kappa = \frac{1}{\sigma^4} \frac{\int C z^4 dz}{\int C dz}, \quad (31)$$

where  $\sigma$  quantifies the width of the profile with

$$\sigma^2 = \frac{\int C z^2 dz}{\int C dz}. \quad (32)$$

For a gaussian profile we have  $\kappa = 3$ , so we always plot  $\kappa - 3$ .

At early times,  $\sigma^2$  increases quadratically with  $t$ , but it soon approaches the linear regime,  $\sigma^2 \sim t$ , until  $\sigma$  saturates at a value comparable to the scale of the box; see Eq. (12).

In Fig. 3 we compare the simulation results for  $\sigma^2$  and  $\kappa - 3$  with those obtained from the model (12) using the same boundary conditions (periodic in  $z$ ) and for the same values of  $u_{\text{rms}}$ . For simplicity we solve Eq. (12) numerically. However, similarly to the cases considered in § III B, we are unable to obtain good fits if we choose exactly the same values of  $k_f$  as in the simulation. Therefore, like in § III B, we treat  $k_f$  as a fit parameter denoted by  $k_f^{(\text{fit})}$ ; see Table II.

There are characteristic departures in the values of  $\sigma^2$  and  $\kappa - 3$  for the model compared with the simulations.

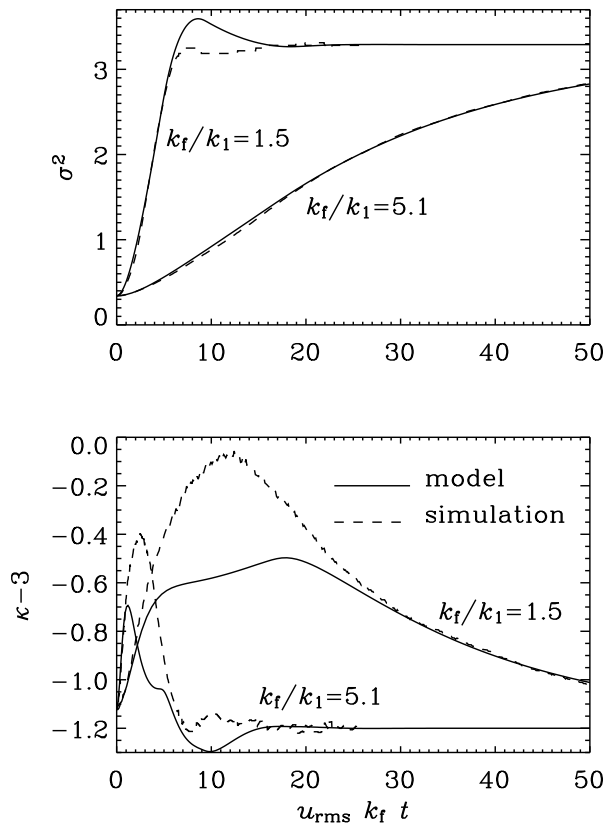


FIG. 3: Comparison of the evolution of  $\sigma^2$  and the kurtosis  $\kappa - 3$  for the non-Fickian diffusion model and the simulation. Note the good agreement at early and late times, but there are departures at intermediate times. The simulations have  $256^3$  meshpoints.

TABLE II: Summary of fit parameters for the initial top hat function experiment. In all cases, the measured value of  $u_{rms} = 0.23$  is used. Note that the values of  $St^{(fit)}$  are the same as those used in § III B, and the values of  $k_f^{(fit)}$  are now slightly closer to  $k_f$  than before.

$k_f/k_1$	$k_f^{(fit)}/k_1$	$St^{(fit)}$
1.5	1.3	1.8
2.2	2.0	1.8
5.1	4.6	2.4

This could perhaps be explained by the fact that, especially when  $k_f/k_1$  is of order unity, the horizontal averages  $\overline{C}$  obtained from the simulations are strongly ‘contaminated’ by a small number of large eddies. Nevertheless, both at early and at late times the agreement between model and simulation is excellent.

The results in § III C confirm our finding of § III B that  $St$  is around 2 (or even larger). Again, this is large enough for oscillatory effects to appear when  $k_f/k_1$  is small.

#### D. Imposed mean concentration gradient

Finally, we consider the case of a uniform gradient in the mean concentration. It is advantageous to split  $C$  into two contributions,

$$C(x, y, z, t) = \rho(x, y, z, t)Gz + c(x, y, z, t), \quad (33)$$

where  $G = \text{const}$  is the imposed mean gradient of the concentration per unit mass (not unit volume). Although  $C$  is now no longer periodic, this choice still preserves periodic boundary conditions for the departure  $c$  from the background profile  $\rho Gz$ . Inserting Eq. (33) into Eq. (20) we have

$$\frac{\partial c}{\partial t} = -\nabla \cdot \left[ \mathbf{U}c - \rho\kappa_C \nabla \left( \frac{c}{\rho} \right) - \rho\kappa_C G \hat{\mathbf{z}} \right] - \rho U_z G, \quad (34)$$

where  $\hat{\mathbf{z}}$  is the unit vector in the  $z$  direction. The main advantage of this setup is the fact that we can now define mean fields by averaging over the entire volume. We denote such averages by angular brackets. Note that  $\langle \mathbf{U} \rangle = 0$ , so  $\mathbf{U} = \mathbf{u}$ . The mean passive scalar flux is then  $\langle u_z c \rangle$  and the triple correlation arising from  $\langle u_z \dot{c} \rangle$  is

$$T_1 = \langle u_z \nabla \cdot (\mathbf{u}c) \rangle. \quad (35)$$

Furthermore, there are triple correlation terms arising from the  $\langle \dot{u}_z c \rangle$  term via the momentum equation. The  $\mathbf{u} \cdot \nabla \mathbf{u}$  term yields the triple correlation

$$T_2 = \langle (\mathbf{u}c) \cdot \nabla u_z \rangle, \quad (36)$$

and the pressure gradient term,  $\nabla p = c_s^2 \nabla \ln \rho$ , yields

$$T_3 = \langle c \nabla_z p \rangle, \quad (37)$$

where  $p = c_s^2 \ln \rho$  can be regarded as a ‘reduced’ pressure and is related to the enthalpy. There is no correlation arising from the forcing term, because the forcing is delta-correlated in time. Furthermore, the contributions from the viscous and diffusive terms are small. Because of periodic boundary conditions,  $T_1 + T_2 = 0$ , so the only contribution surviving from the sum of all three terms is  $T_3$ . Thus, the final expression for  $\tau$  is

$$\tau = \langle u_z c \rangle / \langle c \nabla_z p \rangle. \quad (38)$$

We note however that, on the average, the two contributions from the momentum equations cancel, i.e.  $T_2 + T_3 = 0$ . Therefore it is also possible to calculate  $\tau$  from the contributions of the passive scalar equation alone, i.e.

$$\tau = \langle u_z c \rangle / \langle u_z \nabla \cdot (\mathbf{u}c) \rangle. \quad (39)$$

We have calculated a series of simulations for different values of the Reynolds number as a function of  $k_f$ . However, for a fixed value of  $\nu$ , and since  $k_f$  changes,

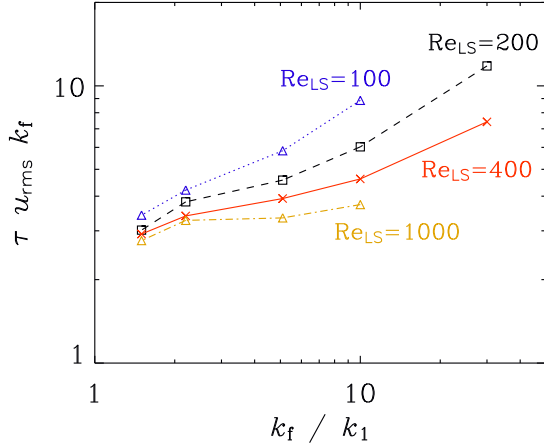


FIG. 4: Strouhal number as a function of  $k_f/k_1$  for different values of  $Re_{LS}$ . The resolution varies between  $64^3$  meshpoints ( $Re_{LS} = 100$ ) and  $512^3$  meshpoints ( $Re_{LS} = 1000$ ).

the Reynolds number, as defined by Eq. (22), is not constant. Therefore we label here the curves by the value of the large scale Reynolds number that we define as

$$Re_{LS} = u_{rms} / (\nu k_1). \quad (40)$$

The result is shown in Fig. 4.

The resulting value of  $St$  depends weakly on  $k_f$  and increases slowly with increasing  $k_f$ . This dependence is weaker for smaller values of  $k_f$ . As the Reynolds number increases, however, the range where  $St$  is approximately constant seems to increase. It is therefore conceivable that  $St$  converges to a universal constant whose value is around 3.

Comparing with the work of Kleorin et al. [17, 18] one has to note that the  $\tau$  approximation was originally formulated in  $k$ -space (see also the early work of Orszag [30]). In Eq. (9), on the other hand, the  $\tau$  approximation is applied directly in real space which may be the reason for minor differences. Nevertheless, under the assumption of Kolmogorov turbulence for  $k > k_f$ , and no turbulence for  $k < k_f$ , one finds that the Strouhal number is unity. Given that there can be further discrepancies arising from differences in the definition of  $St$ , we conclude that their result is in broad agreement with ours.

Since the simulations presented here are weakly compressible, comparison with incompressible theory may not be quite proper. If the assumption of incompressibility is relaxed, i.e.  $\nabla \cdot \mathbf{u} \neq 0$ , there is an extra term,  $-u_i \partial_j u_j \overline{C}$  on the right hand side of Eq. (9). In Eq. (12) this leads to an extra advection term,  $\tau^{-1} \nabla \cdot (\overline{\mathbf{U}}_{\text{eff}} \overline{C})$  on the left hand side. Here,  $\overline{\mathbf{U}}_{\text{eff}} = \overline{\mathbf{U}} - \tau \overline{\mathbf{u} \nabla \cdot \mathbf{u}}$  is a new effective advection velocity; see Refs. [34, 35]. In the simulations presented here, the term  $\overline{\mathbf{u} \nabla \cdot \mathbf{u}}$  is largest when  $k_f/k_1$  is small, but even then it is at most a few percent

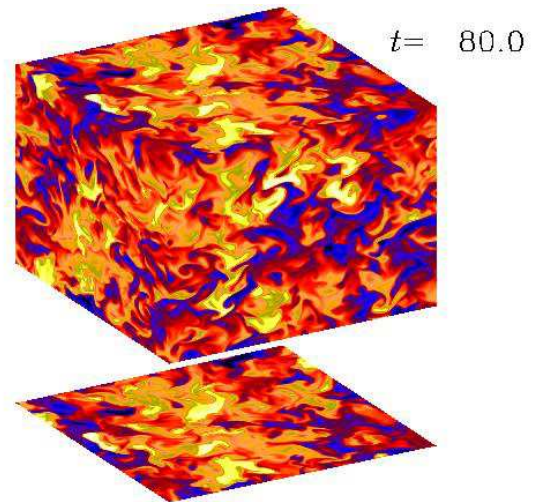


FIG. 5: Visualizations of  $C$  on the periphery of the simulation domain at a time when the simulation has reached a statistically steady state.  $k_f/k_1 = 5.1$ ,  $Re_{LS} = 400$ .

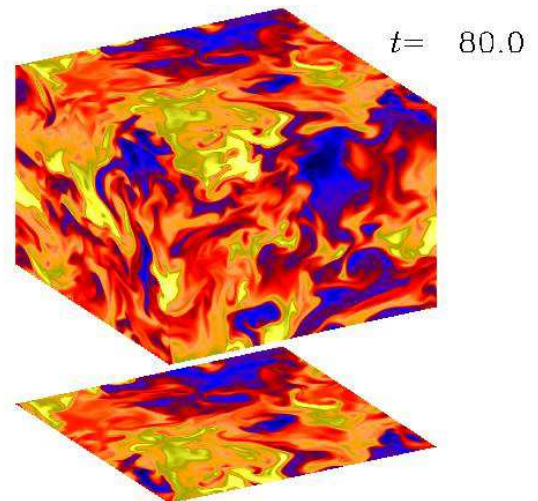


FIG. 6: Same as Fig. 5, but for  $k_f/k_1 = 1.5$ .

of  $u_{rms}^2 k_f$ . This justifies *a posteriori* the neglect of compressibility effects in the interpretation of the numerical results.

Visualizations of  $C$  on the periphery of the simulation domain are shown in Figures 5 and 6 for  $k_f = 5.1$  and  $1.5$ , respectively [41]. Note the combination of large patches (scale  $\sim 1/k_f$ ) together with thin filamentary structures. This is particularly clear in the case with  $k_f/k_1 = 1.5$ . The kinetic energy spectrum is close to  $k^{-5/3}$ , but the passive scalar spectrum is clearly shallower (perhaps like  $k^{-1.4}$ ; see Fig. 7). These spectra are, as usual, integrated over shells of constant  $k \equiv |\mathbf{k}|$  and normalized such that  $\int_0^\infty E_K(k) dk = \frac{1}{2} \langle \mathbf{u}^2 \rangle$  and  $\int_0^\infty E_C(k) dk = \frac{1}{2} \langle c^2 \rangle$ .

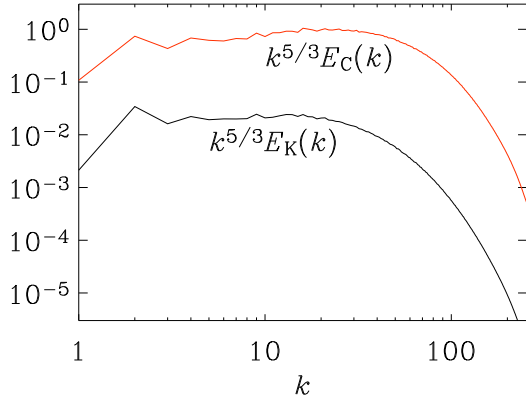


FIG. 7: Compensated kinetic energy and passive scalar spectra for the run with  $k_f/k_1 = 2.2$ ,  $Re_{LS} = 1000$ .

#### IV. CONCLUSIONS

Two important results have emerged from the present investigation. First, the Strouhal number is generally above unity and may have a universal value between 2 and 3 for forced turbulence. This implies that the classical first order smoothing approach is invalid. Second, the triple correlations that are normally neglected are of comparable magnitude to the second order corrections that correspond to the passive scalar flux. The minimal tau approximation in which the two are assumed to be proportional to each other is shown to be justified.

As was shown recently by Blackman and Field in the context of magnetohydrodynamics [14] and then in the context of passive scalar diffusion [15], this leads to an additional time derivative in the mean field equation which then takes the form of a damped wave equation. Our work has now shown that when the forcing occurs on large enough scale ( $k_f \lesssim 2k_1$ ) there is evidence for mildly oscillatory behavior.

Among the various methods for determining the Strouhal number in a turbulence simulation, the approach of imposing a uniform gradient of the passive scalar concentration is the most direct one in that no fitting procedure is needed. Using this approach requires however the firm knowledge that the functional form of the mean field equation is correct. This underlines the importance of the first two approaches where we were able to compare the evolution of various statistical quantities with those obtained by solving the model equation. The only shortcoming here is that we had to find not only the value of the Strouhal number, but we also had to allow  $k_f^{(\text{fit})}$  to deviate (slightly) from the actual value

of  $k_f$ . Although the difference between the two is perhaps not unreasonable, one would like to have some theoretical understanding of this discrepancy.

It is remarkable that in all three experiments the value of the Strouhal number depends only weakly on  $k_f$ . This suggests that the relaxation time  $\tau$  decreases with increasing values of  $k_f$ ; see Eq. (13). We also emphasize that St is similar in all three experiments, even though the wavenumber corresponding to the variation of the mean concentration changed significantly. This suggests that  $\tau$  does not depend on the scale of the concentration, even though such a dependence is in principle being allowed for [18, 19, 30].

The method used in the present paper to determine the Strouhal number from simulations can straightforwardly be applied to magnetohydrodynamics. In that case the magnetic field plays the role of the passive scalar gradient. Both satisfy very similar equations and in both cases a mean field can easily be applied while still retaining fully periodic boundary conditions. In both cases the closure approach of Blackman and Field predicts non-Fickian turbulent diffusion and hence the occurrence of an extra time derivative [14, 15]. Their analytic approach and closure agrees reasonably well with our simulations. Another application would be to determine the role of an extra time derivative in connection with turbulent viscosity. In that case a mean gradient could be imposed using the shearing box approximation [42, 43]. The first two methods described in the present paper should also still be applicable in that case. An obvious question that arises in this connection is whether non-Fickian diffusive properties could also play a role in attempts to find useful subgrid scale models for Large Eddy Simulations. The difficulty here is that one has to deal with averages that do not satisfy the Reynolds rules. Apart from this difficulty there should be no reason why an extra time derivative should not also be incorporated in such simulations.

#### Acknowledgments

We thank Eric Blackman, Nathan Kleorin, and Günther Rüdiger for useful comments on our paper. P.K. acknowledges the financial support from the Magnus Ehrnrooth foundation and the travel support from DFG Graduate School ‘Nonlinear Differential Equations: Modelling, Theory, Numerics, Visualisation’. A.M. acknowledges the financial support from Hans Böckler Stiftung. P.K. and A.M. wish to thank Nordita and its staff for their hospitality during their visits. Use of the parallel computers in Odense (Horseshoe) and Leicester (Ukaff) is acknowledged.

[1] B. Eckhardt and J. Schumacher, “Turbulence and passive scalar transport in a free-slip surface,” *Phys. Rev.* **E 64**,

- [2] T. Elperin, N. Kleeorin, I. Rogachevskii, and D. Sokoloff, "Passive scalar transport in a random flow with a finite renewal time: Mean-field equations," *Phys. Rev.* **E 61**, 2617 (2000).
- [3] H. K. Moffatt *Magnetic Field Generation in Electrically Conducting Fluids*. Cambridge University Press, Cambridge (1978).
- [4] F. Krause and K.-H. Rädler *Mean-Field Magnetohydrodynamics and Dynamo Theory*. Pergamon Press, Oxford (1980).
- [5] P. L. Sulem, Z. S. She, H. Scholl, and U. Frisch, "Generation of large-scale structures in three-dimensional flow lacking parity invariance," *J. Fluid Mech.* **205**, 341 (1989).
- [6] A. Brandenburg and B. v. Rekowski, "Astrophysical significance of the anisotropic kinetic alpha effect," *Astron. Astrophys.* **379**, 1153 (2001).
- [7] G. Rüdiger *Differential rotation and stellar convection: Sun and solar-type stars*. Gordon & Breach, New York (1989).
- [8] L. L. Kitchatinov and G. Rüdiger, "A-effect and differential rotation in stellar convection zones," *Astron. Astrophys.* **276**, 96 (1993).
- [9] J.-P. Bouchaud and A. Georges, "Anomalous diffusion in disordered media: statistical mechanisms, models and physical applications," *Phys. Rep.* **195**, 127 (1990).
- [10] M. S. Miesch, A. Brandenburg, and E. G. Zweibel, "Non-local transport of passive scalars in turbulent penetrative convection," *Phys. Rev.* **E61**, 457 (2000).
- [11] R. B. Stull, "Transilient turbulence theory. Part I: the concept of eddy-mixing across finite distances," *J. Atmos. Sci.* **41**, 3351 (1984).
- [12] R. B. Stull, "Review of transilient turbulence theory and nonlocal mixing," *Boundary Layer Meteorol.* **62**, 21 (1993).
- [13] A. Brandenburg and D. Sokoloff, "Local and nonlocal magnetic diffusion and alpha-effect tensors in shear flow turbulence," *Geophys. Astrophys. Fluid Dynam.* **96**, 319 (2002).
- [14] E. G. Blackman and G. B. Field, "New dynamical mean-field dynamo theory and closure approach," *Phys. Rev. Lett.* **89**, 265007 (2002).
- [15] E. G. Blackman and G. B. Field, "A simple mean field approach to turbulent transport," *Phys. Fluids* **15**, L73 (2003).
- [16] S. I. Vainshtein and L. L. Kitchatinov, "The macroscopic magnetohydrodynamics of inhomogeneously turbulent cosmic plasmas," *Geophys. Astrophys. Fluid Dynam.* **24**, 273 (1983).
- [17] N. I. Kleeorin, I. V. Rogachevskii, and A. A. Ruzmaikin, "Magnetic force reversal and instability in a plasma with advanced magnetohydrodynamic turbulence," *Sov. Phys. JETP* **70**, 878 (1990).
- [18] N. I. Kleeorin, M. Mond, and I. Rogachevskii, "Magnetohydrodynamic turbulence in the solar convective zone as a source of oscillations and sunspots formation," *Astron. Astrophys.* **307**, 293 (1996).
- [19] K.-H. Rädler, N. Kleeorin, and I. Rogachevskii, "The mean electromotive force for MHD turbulence: the case of a weak mean magnetic field and slow rotation," *Geophys. Astrophys. Fluid Dynam.* **97**, 249 (2003).
- [20] M. M. R. Williams, "Neutron transport in spatially random media: An assessment of the accuracy of first order smoothing," *Nucl. Sci. Eng.* **135**, 123 (2000).
- [21] H. T. Chen and J. Y. Lin, "Analysis of 2-dimensional hyperbolic heat-conduction problems," *Int. J. Heat Mass Transfer* **37**, 153 (1994).
- [22] W. Israel, "Gravitational collapse and causality," *Phys. Rev.* **153**, 1388 (1967).
- [23] W. Kley and J. C. B. Papaloizou, "Causal viscosity in accretion disc boundary layers," *Monthly Notices Roy. Astron. Soc.* **285**, 239 (1997).
- [24] M. K. Mak and T. Harko, "Exact causal viscous cosmologies," *Gen. Relativ. Gravit.* **30**, 1171 (1998).
- [25] N. Depireux and G. Lebon, "An extended thermodynamics modeling of non-Fickian diffusion," *J. Non-Newtonian Fluid Mech.* **96**, 105 (2001).
- [26] H. T. Chen and K. C. Liu, "Analysis of non-Fickian diffusion problems in a composite medium," *Comp. Phys. Comm.* **150**, 31 (2003).
- [27] A. M. Weinberg and E. P. Wigner *The physical theory of neutron chain reactors*. University of Chicago Press, Chicago (1958), Chap. 9.
- [28] A. K. Das, "A non-Fickian diffusion equation," *J. Appl. Phys.* **70**, 1355 (1991).
- [29] S. Ghosal and J. B. Keller, "A hyperbolic equation for turbulent diffusion," *Nonlinearity* **13**, 1855 (2000).
- [30] S. A. Orszag, "Analytical theories of turbulence," *J. Fluid Mech.* **41**, 363 (1970).
- [31] M. Lesieur *Turbulence in Fluids*. Martinus Nijhoff Publishers, Dordrecht (1990).
- [32] C. Cattaneo, "On the conduction of heat, Atti Del Seminar," In: Modena 3, Mat. Fis. Univ. p. 3 (1948); see also M. P. Verotte, "Les paradoxes de la theorie continue de l'equation de la chaleur," *Comptes Rendus Acad. Sci.* **246**, p. 3154 (1958).
- [33] T. A. Yousef, A. Brandenburg, and G. Rüdiger, "Turbulent magnetic Prandtl number and magnetic diffusivity quenching from simulations," *Astron. Astrophys.* **411**, 321 (2003).
- [34] T. Elperin, N. Kleeorin, and I. Rogachevskii, "Turbulent thermal diffusion of small inertial particles," *Phys. Rev. Lett.* **76**, 224 (1996).
- [35] T. Elperin, N. Kleeorin, and I. Rogachevskii, "Turbulent barodiffusion, turbulent thermal diffusion, and large-scale instability in gases," *Phys. Rev.* **55**, 2713 (1997).
- [36] For this type of a weakly compressible simulation, we find that the energies of solenoidal and potential components of the flow have a ratio  $E_{\text{pot}}/E_{\text{sol}} \approx 10^{-4}$ - $10^{-2}$  for most scales; only towards the Nyquist frequency the ratio increases to about 0.1. It is thus reasonable to assume that compressibility is irrelevant for the results presented here.
- [37] A. Brandenburg, "The inverse cascade and nonlinear alpha-effect in simulations of isotropic helical hydromagnetic turbulence," *Astrophys. J.* **550**, 824 (2001).
- [38] We use the Pencil Code which is a cache efficient grid based high order code (sixth order in space and third order in time) for solving the compressible MHD equations; [www.nordita.dk/data/brandenb/pencil-code](http://www.nordita.dk/data/brandenb/pencil-code).
- [39] N. E. L. Haugen, A. Brandenburg, and W. Dobler, "Is nonhelical hydromagnetic turbulence peaked at small scales?" *Astrophys. J. Lett.* **597**, L141 (2003).
- [40] W. Dobler, N. E. L. Haugen, T. A. Yousef, and A. Brandenburg, "Bottleneck effect in three-dimensional turbulence simulations," *Phys. Rev.* **E 68**, 026304 (2003).
- [41] Animations can be found on [www.nordita.dk/~brandenb/movies/pscalar](http://www.nordita.dk/~brandenb/movies/pscalar).

- [42] J. F. Hawley, C. F. Gammie, and S. A. Balbus, “Local three-dimensional magnetohydrodynamic simulations of accretion discs,” *Astrophys. J.* **440**, 742 (1995).
- [43] A. Brandenburg, Å. Nordlund, R. F. Stein, and I. Torkelsson, “Dynamo generated turbulence and large scale magnetic fields in a Keplerian shear flow,” *Astrophys. J.* **446**, 741 (1995).